

The role of the dopant in the superconductivity of diamond

X. Blase, Ch. Adessi, D. Connétable

*Laboratoire de Physique de la Matière Condensée et des Nanostructures (LPMCN), CNRS and
Universit Claude Bernard Lyon I, UMR 5586, Btiment Brillouin, 43 Bd du 11 Novembre 1918,
69622 Villeurbanne Cedex, France.*

(February 2, 2008)

Abstract

We present an *ab initio* study of the recently discovered superconductivity of boron doped diamond within the framework of a phonon-mediated pairing mechanism. The role of the dopant, in substitutional position, is unconventional in that half of the coupling parameter λ originates in strongly localized defect-related vibrational modes, yielding a very peaked Eliashberg $\alpha^2 F(\omega)$ function. The electron-phonon coupling potential is found to be extremely large and T_C is limited by the low value of the density of states at the Fermi level.

EFFET ISOTOPIC DU BORE: SUGGERER EXPERIENCE !!

In a recent paper¹, the superconductivity of boron doped (B-doped) diamond was evidenced experimentally with a transition temperature T_C of 4 K. This work follows the discovery of superconductivity in doped silicon clathrates^{2,3} ($T_C=8$ K), a cage-like silicon material which crystallizes in the same sp^3 environment as the diamond phase. Further, the superconductivity of carbon-based clathrates was predicted on the basis of *ab initio* simulations^{3,4}.

Even though the reported temperatures are rather low, the superconducting transition of column IV semiconductors is of much interest as it concerns very common materials. Further, in the case of the carbon clathrates, it has been predicted that the electron-phonon potential $V_{ep}=\lambda/N(E_F)$ (where $N(E_F)$ is the density of states at the Fermi level), may be extremely large^{3,4}. Finally, the superconductivity of hole-doped strongly bonded covalent systems is reminiscent of that of the MgB_2 compound⁵.

As compared to the cage-like clathrate phase, diamond is difficult to dope as the network is much denser. This explains why the superconductivity of doped diamond was never observed, as only quite recently a doping in the limit of a few percent could be achieved. As described in Ref. 1, it is only for a boron concentration $c > 10^{22} \text{ cm}^{-3}$ that a degenerate semiconductor or metallic character can be observed.

In two recent work^{6,7}, a first theoretical study of the superconductivity of B-doped diamond within an elegant virtual crystal approximation was proposed. In this approach, the crystal is made of “averaged carbon-bore atoms” (nuclear charge $Z=(1-x)Z_C + xZ_B$) within the standard 2 atoms/cell structure of diamond, and B atoms are not considered explicitly. As such, the superconductivity of B-doped diamond was analyzed in terms of Bloch-like delocalized electron and phonon “average” states.

In this work, we study by means of *ab initio* calculations the electron-phonon coupling in B-doped diamond. We consider explicitly a large supercell with one B atom in substitution. The metallic character of the doped system is evidenced and the deviations from a simple rigid band model are discussed. We show further that the boron atoms yield very localized

vibrational modes which contribute to half of the electron-phonon coupling parameter λ , in large contrast with the picture conveyed by the virtual crystal approximation. The value of λ is calculated *ab initio*, yielding an unusually large electron-phonon coupling potential V_{ep} or deformation potential D.

Our calculations are performed within the local density approximation to density functional theory⁸ (DFT) and a pseudo-potential⁹ plane-wave approach. A 55 Ryd energy cut-off and a (4x4x4) Monkhorst-Pack¹⁰ sampling of the Brillouin zone (BZ) showed good convergence for structural relaxations. The phonon modes and the electron-phonon (e-ph) coupling matrix elements were obtained within the framework of perturbative DFT¹¹. Due to the computational cost, phonons were calculated at the $\mathbf{q} = \mathbf{\Gamma}$ point only. This is equivalent to a (3x3x3) sampling of the undoped diamond BZ.

For the calculation of the average e-ph matrix elements $g_{q\nu}$ over the Fermi surface, required to evaluate λ :

$$\lambda = N(E_f)V_{ep} = 2N(E_f) \sum_{\mathbf{q}\nu} < |g_{q\nu}|^2 > / \hbar\omega_{q\nu} \quad (1)$$

$$< |g_{q\nu}|^2 > = \int \frac{d^3k}{\Omega_{BZ}} \sum_{n,n'} |g_{q\nu}(kn n')|^2 \frac{\delta(\epsilon_{k+q,n'})\delta(\epsilon_{kn})}{N(E_F)^2} \quad (2)$$

$$g_{q\nu}(kn n') = \left(\frac{\hbar}{2M\omega_{q\nu}}\right)^{1/2} < \psi_{n\mathbf{k}}^0 | \hat{\epsilon}_{\mathbf{q}\nu} \cdot \frac{\delta V}{\delta \hat{u}_{q\nu}} | \psi_{n'\mathbf{k}+\mathbf{q}}^0 > \quad (3)$$

a much larger (8x8x8) \mathbf{k} -point sampling was used. In Eqn. 2, the origin of the electronic energies (ϵ_{kn}) is taken to be the Fermi energy E_F .

Our system consists of a diamond (3x3x3) supercell (54 atoms) with one B atom in substitution (noted BC₅₃ in what follows). We are thus in a 1.85% doping limit, close to the $2.5 \pm 0.5\%$ studied experimentally. Upon structural relaxation, the B-C bond length is 1.57 Å as compared to the 1.54 Å for the C-C bonds in undoped diamond (LDA values). The distance between second and third carbon neighbors is reduced to 1.52 Å in order to accommodate the larger B-C bonds.

We first explore the electronic properties and compare the band structure of BC₅₃ with that of diamond (see Fig. 1). As expected, we are clearly in a metallic regime with the Fermi

level located at ~ 0.54 eV below the top of the valence bands. Even though Fig. 1 seems to confirm the model of rigid band doping around E_F , clear differences exist in particular at the zone boundaries where degeneracies are left due to the reduction of the periodicity under doping. We note that in most directions, the band structure of pure and B-doped diamond start to significantly depart from each other precisely below E_F ¹².

We also calculate the total density of electronic states (eDOS) projected onto the atomic orbitals. Even though the eDOS projected onto the B orbitals (eDOS_B) is small, it is instructive to plot (Fig. 1b) the ratio $N_a \times \text{eDOS}_B / \text{eDOS}$, where $N_a=54$ is the number of atoms per unit cell. Clearly, close to E_F , the relative weight of B orbitals into the wavefunctions is much larger than the weight on any given carbon atom. As expected, this ratio increases where the bands of the ideal and doped diamond differ most significantly. An analysis of the projection of the eigenstates onto the atomic orbital basis shows that the leading coefficients are the (p_x, p_y, p_z) B orbitals¹³. Such results indicate that even though degenerate with the diamond Bloch states, the wavefunctions of interest for e-ph coupling exhibit some degree of localization around the B atom.

We now study the phonon states at Γ . The related DOS ($p\text{DOS}$) is shown in Fig. 2b and compared in Fig. 2a to the one of undoped diamond¹⁴. As compared to the virtual-crystal approximation results, we do not observe the very large softening of the zone-center phonon modes predicted in Ref. 6. However, the splitting of the highest diamond mode (Fig. 2a) clearly results in transferring spectral weight to lower energy. This can be interpreted on the average as a softening of the optical frequencies. In particular, zone-center modes emerge around 1200 cm^{-1} (Fig. 2b) which are consistent with the appearance of new broad peaks in Raman experiments around $1220 \text{ cm}^{-1,15}$.

More insight can be gained by calculating the $p\text{DOS}$ projected onto the B atom and its 4 C neighbors (thick line). The most salient feature is that the new modes (3-fold) at 1024 cm^{-1} (vertical dotted lines in Fig. 2) project to more than 50% on these 5 atoms. The analysis of the associated eigenvectors clearly indicates that these three modes correspond to the stretching of the B to neighboring C atom bonds. The displacement of the B atom is

$\sim 22\%$ larger than that of C neighbors as expected from the difference in masses. Therefore, the dopant atoms induce vibrational modes which are very localized in space. This is a significant deviation from a virtual crystal approach where only extended phonon states can be evidenced. The influence of such modes on the e-ph coupling is now shown to be crucial.

We follow equations 1-3 to calculate λ . With our limited \mathbf{q} -point sampling¹⁶, we find that $\lambda(q = \Gamma)$ is rather sensitive to the gaussian broadening used to mimic the δ -functions in Eq. 2. However, such a variation is primarily related to the variation of the nesting factor $n(q)$ (that can be obtained by setting $g_{q\nu}(knn')$ to unity in Eq. 2). This factor $n(q)$ is a measure of phase space availability for electron scattering by phonons. Indeed, one verifies that the quantity $\lambda(q)/n(q)$ ($q=\Gamma$) is much more stable and displays a plateau over a large energy broadening range. We thus define an averaged λ by rewriting:

$$\begin{aligned}\lambda &= \int d^3q \lambda(q) = \int d^3q n(q) \lambda(q)/n(q) \\ &\sim \lambda(\Gamma)/n(\Gamma) \int d^3q n(q) = N(E_F)^2 \lambda(\Gamma)/n(\Gamma)\end{aligned}$$

Such an approximation relies on the usual assumption that the e-ph matrix elements are varying much more smoothly as a function of \mathbf{q} than the nesting factor.

We find $\lambda=0.43 \pm 0.01$. Such a value of λ is much smaller than that of MgB_2 (in the absence of anharmonic effects¹⁷, $\lambda(\text{MgB}_2) \sim 1$). Assuming now that the McMillan expansion¹⁸ is valid in the limit of degenerate semiconductors:

$$T_c = \frac{\hbar\omega_{log}}{1.2k_B} \exp \left[\frac{-1.04(1 + \lambda)}{\lambda - \mu^*(1 + 0.62\lambda)} \right]$$

and with a logarithmic averaged phonon frequency ω_{log} of 1023 cm^{-1} , the screening parameter μ^* needed to reproduce the 4 K experimental value of T_C is found to be of the order of 0.13-0.14¹⁹. This is a very standard value, indicating that phonon-mediated pairing mechanisms can adequately account for the superconducting transition in impurity-doped diamond.

With $N(E_F)=20.8 \text{ states/spin/Ry/Cell}$, the e-ph potential V_{ep} is $280 \text{ meV} \pm 10 \text{ meV}$. Such a value is comparable to what was found in the Li-doped carbon clathrates ($V_{ep} \sim 250$

meV⁴) and much larger than the 60-70 meV found for the fullerenes²⁰. This was analyzed in terms of the amount of sp^3 character of the C-C bonds³. For sake of comparison with Refs. 6, 7, we calculate the deformation potential D such that $\lambda = N_2 D^2 / M \omega^2$, where N_2 is the eDOS in eV/state/spin/“2 atoms cell”. With $N_2 = 0.057$ and $\omega = 1023 \text{ cm}^{-1}$, one finds $D = 27 \text{ eV/\AA}^{-1}$, larger than the $D \sim 21 \text{ eV/\AA}^{-1}$ value found in the virtual crystal approximation^{6,7}. This value is more than twice as large as the one calculated for MgB_2 , indicating that it is primarily the low density of states at the Fermi level, related to the 3D nature of diamond, that is responsible for the low value of λ and T_c .

Better \mathbf{q} -point sampling and the influence of anharmonicity^{6,17} will certainly change the value of λ . Beyond the numerical estimates, it is important to look at the spectral decomposition of λ , that is the Eliashberg function $\alpha^2 F(\omega)$ (Fig. 2c):

$$\alpha^2 F(\omega) = \frac{1}{2} \sum_{\mathbf{q}\nu} \omega_{\mathbf{q}\nu} \lambda_{\mathbf{q}\nu} \delta(\omega - \omega_{\mathbf{q}\nu}) \quad (4)$$

By comparison with the p DOS, it appears that a significant contribution to λ comes from the B-related phonon modes. *As a matter of fact, these 3 modes contribute to about 50% of the coupling*²¹. In particular, the resulting Eliashberg function is very peaked at the impurity vibrational modes energy, displaying a δ -like shape. Therefore, not only the density of states $N(E_F)$, but also the strength of the e-ph coupling, can be tailored by changing the dopant concentration and/or chemical type. This mechanism offers thus an additional flexibility in trying to increase T_c . The situation is very different from the one of fullerenes or clathrates where the low frequency phonon modes associated with the dopant hardly contribute to λ .

To strengthen that point, we look at the superconductivity of diamond within a rigid band model²². We plot in Fig. 3 the evolution of λ as a function of the position of the Fermi level. For E_f located ~ 0.5 - 0.6 eV below the top of the valence bands, we find a λ of ~ 0.24 , that is roughly 55% of what we find in the BC_{53} case. Even though very qualitative, this computer experiment substantiates the conclusion that B-related modes contribute significantly to the e-ph coupling. Further, Fig. 3 clearly suggests that larger λ could be achieved under larger doping conditions due to the quadratic rise of $N(E_F)$ as a

function of E_F .

It is certainly accidental that just half of the coupling originates in B-modes as the weight of the eigenstates on the dopant should scale as $\sqrt{N_a}$ under varying concentration (neglecting the electronic localization effect described above). In addition, the simple structural model studied here does not account for the effect of randomness, nor the possibility for B atoms to cluster or adopt other configurations. It is clear however that the role of the dopant cannot be interpreted solely as providing charges to the network, nor as softening the phonon modes by depleting the bonding states at the top of the valence bands. In particular, such results reveal that any attempt to explain the superconductivity of doped diamond within a rigid band model or the virtual-crystal approximation should be taken with care. The importance of the impurity related vibrational modes is expected to be very general and should apply to any semiconductor/insulator doped by strongly bound atoms.

In conclusion, we have shown that the role of boron in doped diamond is unconventional in that a significant fraction of the coupling coefficient λ originates in vibrational modes very localized on the defect centers. With a λ of 0.43, much smaller than that of $\text{MgB}_2 \sim 1$, T_C remains small. Even though the electron-phonon potential is extremely large, the 3D nature of the network reduces the density of states at the Fermi level. This invites to study the case of doped diamond surfaces where both the contraction of the reconstructed bonds and the 2D nature of the surface states may lead to much larger T_C ²³.

Acknowledgements: Calculations have been performed at the French CNRS national computer center at IDRIS (Orsay). The authors are indebted to région Rhône-Alpes for financial support through the “Thématique prioritaire programme 2003-2005” in Material Sciences.

REFERENCES

- ¹ E.A. Ekimov *et al.*, *Nature* **428**, 642 (2004).
- ² H. Kawaji, H.-O. Horie, S. Yamanaka, and M. Ishikawa, *Phys. Rev. Lett.* **74**, 1427 (1995);
K. Tanigaki *et al.*, *Nature Materials* **2**, 653 (2003).
- ³ D. Connétable *et al.*, *Phys. Rev. Lett.* **91**, 247001 (2003).
- ⁴ I. Spagnolatti, M. Bernasconi, G. Benedek, *Eur. Phys. J. B* **34**, 63 (2003).
- ⁵ J. Nagamatsu *et al.*, *Nature* (London) **410**, 63 (2001).
- ⁶ L. Boeri, J. Kortus, O.K. Andersen, cond-mat/0404447.
- ⁷ K.W. Lee and W.E. Pickett, cond-mat/0404547.
- ⁸ P. Hohenberg and W. Kohn, *Phys. Rev. B* **136**, 864 (1964); D.M. Ceperley and B.J. Alder, *Phys.Rev.Lett.* **45**, 566 (1980).
- ⁹ N. Troullier and J. L. Martins, *Phys. Rev. B* **43**, 1993 (1991); K. Kleinman and D.M. Bylander, *Phys. Rev. B* **48**, 1425 (1982).
- ¹⁰ H.J. Monkhorst and J.D. Pack, *Phys. Rev. B* **13**, 5188 (1976).
- ¹¹ S. Baroni, S. de Gironcoli, A. Dal Corso, and P. Giannozzi, *Rev. Mod. Phys.* **73** (2), 515 (2001); S. Baroni, A. Dal Corso, S. de Gironcoli, and P. Giannozzi, <http://www.pwscf.org>.
- ¹² Similar results have been obtained for heavily doped BC_x graphitic systems with, in the x=3 case, a complete depletion of the π bands. See: Y. Miyamoto *et al.*, *Phys. Rev. B* **50**, 18360 (1994).
- ¹³ Typically, more than 99% of the wavefunctions total weight projects onto the atomic orbitals suggesting a very small “spilling” factor. See: Sanchez-Portal *et al.*, *Sol. State Commun.* **95**, 685 (1995).
- ¹⁴ For undoped diamond, we use the conventional 2 atoms/cell structure with a (3x3x3)

\mathbf{q} -grid which folds onto the Γ point of the (3x3x3) cell.

¹⁵ R.J. Zhang, S.T. Lee, Y.W. Lam, *Diamond. Relat. Mater.* **5**, 1288 (1996).

¹⁶ In the limit of low doping, and as emphasized in Refs. 6, 7, zone-center optical phonons are expected to contribute primarily to the e-ph coupling. Such an approximation is at the heart of the $\mathbf{q}=\Gamma$ deformation potential approach developed by Lee and Pickett in Ref. 7.

¹⁷ H.J. Choi *et al.*, *Nature* (London) **418**, 758 (2002); *ibid*, *Phys. Rev. B* **66**, 020513 (2002); Michele Lazzeri, Matteo Calandra, and Francesco Mauri, *Phys. Rev. B* **68**, 220509(R) (2003).

¹⁸ W.L. McMillan, *Phys. Rev.* **167**, 331 (1968).

¹⁹ Using the modified McMillan formula proposed in Ref. 6 for δ -shaped Eliashberg functions (see Fig. 2c), we find a μ^* of 0.13 for $\omega=1023\text{ cm}^{-1}$ in good agreement with the standard formulation used in the text.

²⁰ O. Gunnarsson, *Rev. Mod. Phys.* **69**, 575-606 (1997).

²¹ This explains in particular that ω_{log} is found to be close to these modes energy.

²² We calculate the phonon and electronic state of pristine diamond (2 atoms/cell) and look at the e-ph coupling for a Fermi level located arbitrarily above and below the band gap. A (30x30x30) and (8x8x8) grid for the \mathbf{k} -point and \mathbf{q} -points was used at convergency.

²³ The electronic properties of n -type doped diamond surfaces and clathrates was studied in the context of obtaining “negative” work function materials for field-emission devices. See e.g.: Warren E. Pickett, *Phys. Rev. Lett.* **73**, 1664 (1994); V. Timoshevskii, D. Connétable, X. Blase, *Appl. Phys. Lett.* **80**, 1385 (2002).

FIGURES

FIG. 1. (a) Details of the top of the valence bands along high-symmetry directions of the FCC BZ for undoped diamond in the (3x3x3) cell (dotted lines) and the doped BC₅₃ system (full lines). The horizontal line is the position of the Fermi level in the doped case. The two band structures have been aligned at the top of the valence bands. (b) Ratio of the density of states projected onto the B-orbitals to the total density of states per atom in the unit cell (this ratio has been set to zero in the band gap).

FIG. 2. Phonon density of states $pDOS$ for (a) bare diamond with modes on an unshifted (3x3x3) grid (b) the boron doped BC₅₃ cell with modes at Γ . In (c) the spectral function $\alpha^2F(\omega)$ is represented for modes at Γ . Energies are in cm^{-1} and the y-axis magnitude is arbitrary. A 5 cm^{-1} broadening has been used. The vertical dotted lines indicate the energy position of the 3-fold B-related vibrational modes.

FIG. 3. Evolution of λ for diamond, doped within a rigid band model (see text), as a function of the Fermi energy position E_F . The energy reference has been set to the top of the valence bands.

The role of the dopant in the superconductivity of diamond

X. Blase, Ch. Adessi, D. Connétable

Laboratoire de Physique de la Matière Condensée et des Nanostructures (LPMCN), CNRS and Université Claude Bernard
Lyon I, UMR 5586, Bâtiment Brillouin, 43 Bd du 11 Novembre 1918, 69622 Villeurbanne Cedex, France.

(February 2, 2008)

We present an *ab initio* study of the recently discovered superconductivity of boron doped diamond within the framework of a phonon-mediated pairing mechanism. The role of the dopant, in substitutional position, is unconventional in that half of the coupling parameter λ originates in strongly localized defect-related vibrational modes, yielding a very peaked Eliashberg $\alpha^2 F(\omega)$ function. The electron-phonon coupling potential is found to be extremely large and T_C is limited by the low value of the density of states at the Fermi level.

In a recent paper [1], the superconductivity of boron doped (B-doped) diamond was evidenced experimentally with a transition temperature T_C of 4 K. This work follows the discovery of superconductivity in doped silicon clathrates [2,3] ($T_C=8$ K), a cage-like silicon material which crystallizes in the same sp^3 environment as the diamond phase. Further, the superconductivity of carbon-based clathrates was predicted on the basis of *ab initio* simulations [3,4].

Even though the reported temperatures are rather low, the superconducting transition of column IV semiconductors is of much interest as it concerns very common materials. Further, in the case of the carbon clathrates, it has been predicted that the electron-phonon potential $V_{ep}=\lambda/N(E_F)$ (where $N(E_F)$ is the density of states at the Fermi level), may be extremely large [3,4]. Finally, the superconductivity of hole-doped strongly bonded covalent systems is reminiscent of that of the MgB_2 compound [5].

As compared to the cage-like clathrate phase, diamond is difficult to dope as the network is much denser. This explains why the superconductivity of doped diamond was never observed, as only quite recently a doping in the limit of a few percent could be achieved. As described in Ref. [1], it is only for a boron concentration $c > 10^{22} \text{ cm}^{-3}$ that a degenerate semiconductor or metallic character can be observed.

In two recent work [6,7], a first theoretical study of the superconductivity of B-doped diamond within an elegant virtual crystal approximation was proposed. In this approach, the crystal is made of “averaged carbon-bore atoms” (nuclear charge $Z=(1-x)Z_C + xZ_B$) within the standard 2 atoms/cell structure of diamond, and B atoms are not considered explicitly. As such, the superconductivity of B-doped diamond was analyzed in terms of Bloch-like delocalized electron and phonon “average” states.

In this work, we study by means of *ab initio* calculations the electron-phonon coupling in B-doped diamond.

We consider explicitly a large supercell with one B atom in substitution. The metallic character of the doped system is evidenced and the deviations from a simple rigid band model are discussed. We show further that the boron atoms yield very localized vibrational modes which contribute to half of the electron-phonon coupling parameter λ , in large contrast with the picture conveyed by the virtual crystal approximation. The value of λ is calculated *ab initio*, yielding an unusually large electron-phonon coupling potential V_{ep} or deformation potential D .

Our calculations are performed within the local density approximation to density functional theory [8] (DFT) and a pseudo-potential [9] plane-wave approach. A 55 Ryd energy cut-off and a (4x4x4) Monkhorst-Pack [10] sampling of the Brillouin zone (BZ) showed good convergence for structural relaxations. The phonon modes and the electron-phonon (e-ph) coupling matrix elements were obtained within the framework of perturbative DFT [11]. Due to the computational cost, phonons were calculated at the $\mathbf{q} = \mathbf{\Gamma}$ point only. This is equivalent to a (3x3x3) sampling of the undoped diamond BZ.

For the calculation of the average e-ph matrix elements $g_{q\nu}$ over the Fermi surface, required to evaluate λ :

$$\lambda = N(E_F)V_{ep} = 2N(E_F) \sum_{\mathbf{q}\nu} < |g_{q\nu}|^2 > / \hbar\omega_{q\nu} \quad (1)$$

$$< |g_{q\nu}|^2 > = \int \frac{d^3k}{\Omega_{BZ}} \sum_{n,n'} |g_{q\nu}(knn')|^2 \frac{\delta(\epsilon_{k+q,n'})\delta(\epsilon_{kn})}{N(E_F)^2} \quad (2)$$

$$g_{q\nu}(knn') = \left(\frac{\hbar}{2M\omega_{q\nu}}\right)^{1/2} < \psi_{n\mathbf{k}}^0 | \hat{\epsilon}_{\mathbf{q}\nu} \cdot \frac{\delta V}{\delta \hat{u}_{q\nu}} | \psi_{n'\mathbf{k}+\mathbf{q}}^0 > \quad (3)$$

a much larger (8x8x8) \mathbf{k} -point sampling was used. In Eqn. 2, the origin of the electronic energies (ϵ_{kn}) is taken to be the Fermi energy E_F .

Our system consists of a diamond (3x3x3) supercell (54 atoms) with one B atom in substitution (noted BC₅₃ in what follows). We are thus in a 1.85% doping limit, close to the $2.5 \pm 0.5\%$ studied experimentally. Upon

structural relaxation, the B-C bond length is 1.57 Å as compared to the 1.54 Å for the C-C bonds in undoped diamond (LDA values). The distance between second and third carbon neighbors is reduced to 1.52 Å in order to accommodate the larger B-C bonds.

We first explore the electronic properties and compare the band structure of BC₅₃ with that of diamond (see Fig. 1). As expected, we are clearly in a metallic regime with the Fermi level located at ~ 0.54 eV below the top of the valence bands. Even though Fig. 1 seems to confirm the model of rigid band doping around E_F , clear differences exist in particular at the zone boundaries where degeneracies are left due to the reduction of the periodicity under doping. We note that in most directions, the band structure of pure and B-doped diamond start to significantly depart from each other precisely below E_F [12].

We also calculate the total density of electronic states (eDOS) projected onto the atomic orbitals. Even though the eDOS projected onto the B orbitals (eDOS_B) is small, it is instructive to plot (Fig. 1b) the ratio $N_a \times \text{eDOS}_B / \text{eDOS}$, where $N_a=54$ is the number of atoms per unit cell. Clearly, close to E_F , the relative weight of B orbitals into the wavefunctions is much larger than the weight on any given carbon atom. As expected, this ratio increases where the bands of the ideal and doped diamond differ most significantly. An analysis of the projection of the eigenstates onto the atomic orbital basis shows that the leading coefficients are the (p_x, p_y, p_z) B orbitals [13]. Such results indicate that even though degenerate with the diamond Bloch states, the wavefunctions of interest for e-ph coupling exhibit some degree of localization around the B atom.

We now study the phonon states at Γ . The related DOS (p DOS) is shown in Fig. 2b and compared in Fig. 2a to the one of undoped diamond [14]. As compared to the virtual-crystal approximation results, we do not observe the very large softening of the zone-center phonon modes predicted in Ref. [6]. However, the splitting of the highest diamond mode (Fig. 2a) clearly results in transferring spectral weight to lower energy. This can be interpreted on the average as a softening of the optical frequencies. In particular, zone-center modes emerge around 1200 cm⁻¹ (Fig. 2b) which are consistent with the appearance of new broad peaks in Raman experiments around 1220 cm⁻¹ [1,15].

More insight can be gained by calculating the p DOS projected onto the B atom and its 4 C neighbors (thick line). The most salient feature is that the new modes (3-fold) at 1024 cm⁻¹ (vertical dotted lines in Fig. 2) project to more than 50% on these 5 atoms. The analysis of the associated eigenvectors clearly indicates that these three modes correspond to the stretching of the B to neighboring C atom bonds. The displacement of the B atom is $\sim 22\%$ larger than that of C neighbors as expected from the difference in masses. Therefore, the

dopant atoms induce vibrational modes which are very localized in space. This is a significant deviation from a virtual crystal approach where only extended phonon states can be evidenced. The influence of such modes on the e-ph coupling is now shown to be crucial.

We follow equations 1-3 to calculate λ . With our limited \mathbf{q} -point sampling [16], we find that $\lambda(q = \Gamma)$ is rather sensitive to the gaussian broadening used to mimic the δ -functions in Eq. 2. However, such a variation is primarily related to the variation of the nesting factor $n(q)$ (that can be obtained by setting $g_{q\nu}(knn')$ to unity in Eq. 2). This factor $n(q)$ is a measure of phase space availability for electron scattering by phonons. Indeed, one verifies that the quantity $\lambda(q)/n(q)$ ($q=\Gamma$) is much more stable and displays a plateau over a large energy broadening range. We thus define an averaged λ by rewriting:

$$\begin{aligned} \lambda &= \int d^3q \lambda(q) = \int d^3q n(q) \lambda(q)/n(q) \\ &\sim \lambda(\Gamma)/n(\Gamma) \int d^3q n(q) = N(E_F)^2 \lambda(\Gamma)/n(\Gamma) \end{aligned}$$

Such an approximation relies on the usual assumption that the e-ph matrix elements are varying much more smoothly as a function of \mathbf{q} than the nesting factor.

We find $\lambda=0.43 \pm 0.01$. Such a value of λ is much smaller than that of MgB₂ (in the absence of anharmonic effects [17], $\lambda(\text{MgB}_2) \sim 1$). Assuming now that the McMillan expansion [18] is valid in the limit of degenerate semiconductors:

$$T_c = \frac{\hbar\omega_{log}}{1.2k_B} \exp \left[\frac{-1.04(1+\lambda)}{\lambda - \mu^*(1+0.62\lambda)} \right]$$

and with a logarithmic averaged phonon frequency ω_{log} of 1023 cm⁻¹, the screening parameter μ^* needed to reproduce the 4 K experimental value of T_C is found to be of the order of 0.13-0.14 [19]. This is a very standard value, indicating that phonon-mediated pairing mechanisms can adequately account for the superconducting transition in impurity-doped diamond.

With $N(E_F)=20.8$ states/spin/Ry/Cell, the e-ph potential V_{ep} is 280 meV \pm 10 meV. Such a value is comparable to what was found in the Li-doped carbon clathrates ($V_{ep} \sim 250$ meV [4]) and much larger than the 60-70 meV found for the fullerenes [20]. This was analyzed in terms of the amount of sp^3 character of the C-C bonds [3]. For sake of comparison with Refs. [6,7], we calculate the deformation potential D such that $\lambda=N_2 D^2/M\omega^2$, where N_2 is the eDOS in eV/state/spin/"2 atoms cell". With $N_2=0.057$ and $\omega=1023$ cm⁻¹, one finds $D = 27$ eV/Å⁻¹, larger than the $D \sim 21$ eV/Å⁻¹ value found in the virtual crystal approximation [6,7]. This value is more than twice as large as the one calculated for MgB₂, indicating that it is primarily the low density of states at the Fermi level,

related to the 3D nature of diamond, that is responsible for the low value of λ and T_C .

Better \mathbf{q} -point sampling and the influence of anharmonicity [6,17] will certainly change the value of λ . Beyond the numerical estimates, it is important to look at the spectral decomposition of λ , that is the Eliashberg function $\alpha^2 F(\omega)$ (Fig. 2c):

$$\alpha^2 F(\omega) = \frac{1}{2} \sum_{\mathbf{q}\nu} \omega_{\mathbf{q}\nu} \lambda_{\mathbf{q}\nu} \delta(\omega - \omega_{\mathbf{q}\nu}) \quad (4)$$

By comparison with the p DOS, it appears that a significant contribution to λ comes from the B-related phonon modes. *As a matter of fact, these 3 modes contribute to about 50% of the coupling* [21]. In particular, the resulting Eliashberg function is very peaked at the impurity vibrational modes energy, displaying a δ -like shape. Therefore, not only the density of states $N(E_F)$, but also the strength of the e-ph coupling, can be tailored by changing the dopant concentration and/or chemical type. This mechanism offers thus an additional flexibility in trying to increase T_C . The situation is very different from the one of fullerenes or clathrates where the low frequency phonon modes associated with the dopant hardly contribute to λ .

To strengthen that point, we look at the superconductivity of diamond within a rigid band model [22]. We plot in Fig. 3 the evolution of λ as a function of the position of the Fermi level. For E_f located ~ 0.5 - 0.6 eV below the top of the valence bands, we find a λ of ~ 0.24 , that is roughly 55% of what we find in the BC_{53} case. Even though very qualitative, this computer experiment substantiates the conclusion that B-related modes contribute significantly to the e-ph coupling. Further, Fig. 3 clearly suggests that larger λ could be achieved under larger doping conditions due to the quadratic rise of $N(E_F)$ as a function of E_F .

It is certainly accidental that just half of the coupling originates in B-modes as the weight of the eigenstates on the dopant should scale as $\sqrt{N_a}$ under varying concentration (neglecting the electronic localization effect described above). In addition, the simple structural model studied here does not account for the effect of randomness, nor the possibility for B atoms to cluster or adopt other configurations. It is clear however that the role of the dopant cannot be interpreted solely as providing charges to the network, nor as softening the phonon modes by depleting the bonding states at the top of the valence bands. In particular, such results reveal that any attempt to explain the superconductivity of doped diamond within a rigid band model or the virtual-crystal approximation should be taken with care. The importance of the impurity related vibrational modes is expected to be very general and should apply to any semiconductor/insulator doped by strongly bound atoms.

In conclusion, we have shown that the role of boron

in doped diamond is unconventional in that a significant fraction of the coupling coefficient λ originates in vibrational modes very localized on the defect centers. With a λ of 0.43, much smaller than that of $\text{MgB}_2 \sim 1$, T_C remains small. Even though the electron-phonon potential is extremely large, the 3D nature of the network reduces the density of states at the Fermi level. This invites to study the case of doped diamond surfaces where both the contraction of the reconstructed bonds and the 2D nature of the surface states may lead to much larger T_C [23].

Acknowledgements: Calculations have been performed at the French CNRS national computer center at IDRIS (Orsay). The authors are indebted to région Rhône-Alpes for financial support through the “Thématique prioritaire programme 2003-2005” in Material Sciences.

-
- [1] E.A. Ekimov *et al.*, *Nature* **428**, 642 (2004).
 - [2] H. Kawaji, H.-O. Horie, S. Yamanaka, and M. Ishikawa, *Phys. Rev. Lett.* **74**, 1427 (1995); K. Tanigaki *et al.*, *Nature Materials* **2**, 653 (2003).
 - [3] D. Connétable *et al.*, *Phys. Rev. Lett.* **91**, 247001 (2003).
 - [4] I. Spagnolatti, M. Bernasconi, G. Benedek, *Eur. Phys. J. B* **34**, 63 (2003).
 - [5] J. Nagamatsu *et al.*, *Nature* (London) **410**, 63 (2001).
 - [6] L. Boeri, J. Kortus, O.K. Andersen, cond-mat/0404447.
 - [7] K.W. Lee and W.E. Pickett, cond-mat/0404547.
 - [8] P. Hohenberg and W. Kohn, *Phys. Rev. B* **136**, 864 (1964); D.M. Ceperley and B.J. Alder, *Phys. Rev. Lett.* **45**, 566 (1980).
 - [9] N. Troullier and J. L. Martins, *Phys. Rev. B* **43**, 1993 (1991); K. Kleinman and D.M. Bylander, *Phys. Rev. B* **48**, 1425 (1982).
 - [10] H.J. Monkhorst and J.D. Pack, *Phys. Rev. B* **13**, 5188 (1976).
 - [11] S. Baroni, S. de Gironcoli, A. Dal Corso, and P. Giannozzi, *Rev. Mod. Phys.* **73** (2), 515 (2001); S. Baroni, A. Dal Corso, S. de Gironcoli, and P. Giannozzi, <http://www.pwscf.org>.
 - [12] Similar results have been obtained for heavily doped BC_x graphitic systems with, in the $x=3$ case, a complete depletion of the π bands. See: Y. Miyamoto *et al.*, *Phys. Rev. B* **50**, 18360 (1994).
 - [13] Typically, more than 99% of the wavefunctions total weight projects onto the atomic orbitals suggesting a very small “spilling” factor. See: Sanchez-Portal *et al.*, *Sol. State Commun.* **95**, 685 (1995).
 - [14] For undoped diamond, we use the conventional 2 atoms/cell structure with a $(3 \times 3 \times 3)$ \mathbf{q} -grid which folds onto the Γ point of the $(3 \times 3 \times 3)$ cell.
 - [15] R.J. Zhang, S.T. Lee, Y.W. Lam, *Diamond. Relat. Mater.* **5**, 1288 (1996).
 - [16] In the limit of low doping, and as emphasized in

- Refs. [6,7], zone-center optical phonons are expected to contribute primarily to the e-ph coupling. Such an approximation is at the heart of the $q=\Gamma$ deformation potential approach developed by Lee and Pickett in Ref. [7].
- [17] H.J. Choi *et al.*, *Nature* (London) **418**, 758 (2002); *ibid*, Phys. Rev. B **66**, 020513 (2002); Michele Lazzeri, Matteo Calandra, and Francesco Mauri, Phys. Rev. B **68**, 220509(R) (2003).
- [18] W.L. McMillan, Phys. Rev. **167**, 331 (1968).
- [19] Using the modified McMillan formula proposed in Ref. [6] for δ -shaped Eliashberg functions (see Fig. 2c), we find a μ^* of 0.13 for $\omega=1023\text{ cm}^{-1}$ in good agreement with the standard formulation used in the text.
- [20] O. Gunnarsson, Rev. Mod. Phys. **69**, 575-606 (1997).
- [21] This explains in particular that ω_{log} is found to be close to these modes energy.
- [22] We calculate the phonon and electronic state of pristine diamond (2 atoms/cell) and look at the e-ph coupling for a Fermi level located arbitrarily above and below the band gap. A $(30 \times 30 \times 30)$ and $(8 \times 8 \times 8)$ grid for the \mathbf{k} -point and \mathbf{q} -points was used at convergence.
- [23] The electronic properties of n -type doped diamond surfaces and clathrates was studied in the context of obtaining “negative” work function materials for field-emission devices. See e.g.: Warren E. Pickett, Phys. Rev. Lett. **73**, 1664 (1994); V. Timoshevskii, D. Connétable, X. Blase, Appl. Phys. Lett. **80**, 1385 (2002).

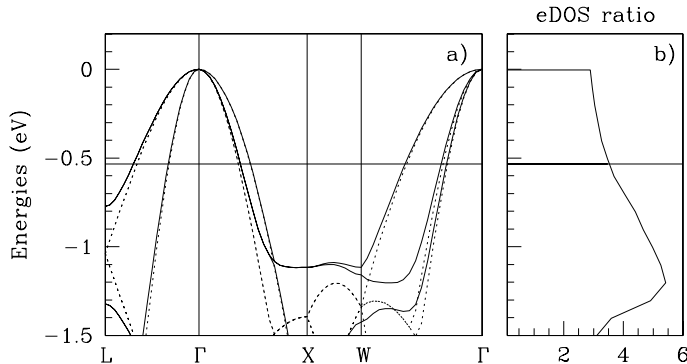


FIG. 1. (a) Details of the top of the valence bands along high-symmetry directions of the FCC BZ for undoped diamond in the $(3 \times 3 \times 3)$ cell (dotted lines) and the doped BC_{53} system (full lines). The horizontal line is the position of the Fermi level in the doped case. The two band structures have been aligned at the top of the valence bands. (b) Ratio of the density of states projected onto the B-orbitals to the total density of states per atom in the unit cell (this ratio has been set to zero in the band gap).

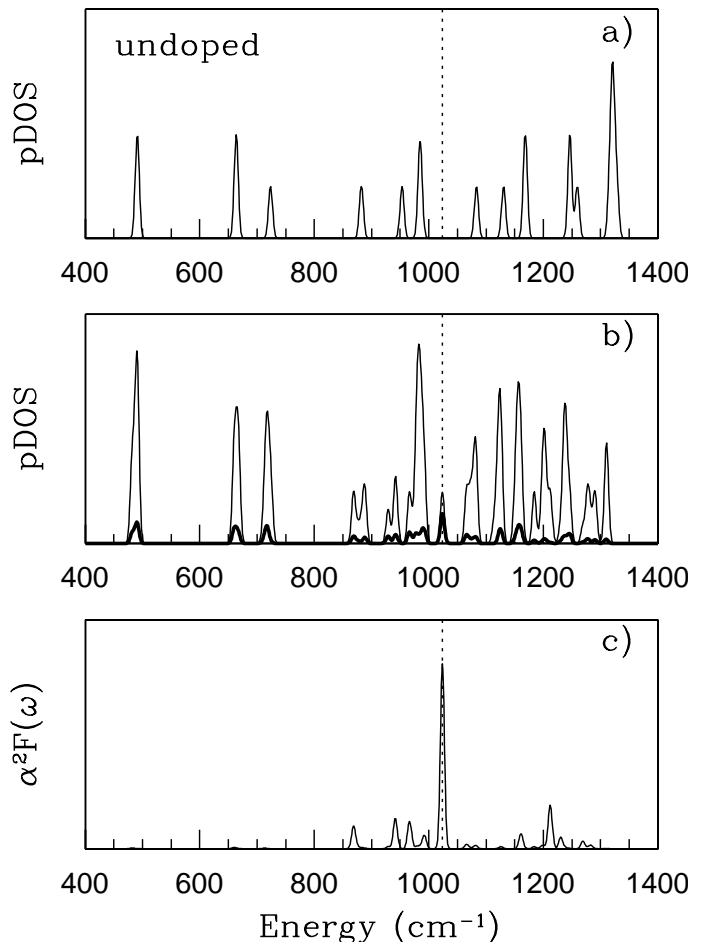


FIG. 2. Phonon density of states $p\text{DOS}$ for (a) bare diamond with modes on an unshifted $(3 \times 3 \times 3)$ grid (b) the boron doped BC_{53} cell with modes at Γ . In (c) the spectral function $\alpha^2 F(\omega)$ is represented for modes at Γ . Energies are in cm^{-1} and the y-axis magnitude is arbitrary. A 5 cm^{-1} broadening has been used. The vertical dotted lines indicate the energy position of the 3-fold B-related vibrational modes.

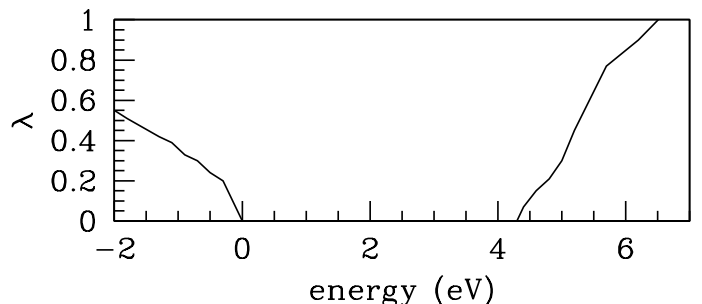


FIG. 3. Evolution of λ for diamond, doped within a rigid band model (see text), as a function of the Fermi energy position E_F . The energy reference has been set to the top of the valence bands.